A new class of sulfur bridged ruthenium–molybdenum complexes, $(L)_2Ru^{II}(\mu\text{-}S)_2Mo^{IV}(OH)_2$ [L=NC_5H_4N=NC_6H_4(R), R=H, *o*-Me/Cl, *m*-Me/Cl]. Synthesis, spectroscopic and electron-transfer properties

Ramapati Samanta, Pradip Munshi, Bidyut Kumar Santra, Goutam Kumar Lahiri*

Department of Chemistry, Indian Institute of Technology, Bombay, Powai, Mumbai-400076, India

Abstract

The reaction of $(NH_4)_2Mo^{VI}S_4$ with the complexes *ctc*-$Ru^{II}(L)_2Cl_2$ (1a–1e) [L=NC_5H_4N=NC_6H_4(R), R=H, *o*-Me/Cl, *m*-Me/Cl; *ctc*=*cis–trans–cis* with respect to chlorides, pyridine and azo nitrogens respectively] in MeOH–H_2O (1:1) resulted in a group of stable sulfur bridged ruthenium–molybdenum complexes of the type $(L)_2Ru^{II}(\mu\text{-}S)_2Mo^{IV}(OH)_2$ (2a–2e). In complexes 2 the terminal Mo=S bonds of the $Mo^{VI}S_4^{2-}$ unit get hydroxylated and the molybdenum ion is reduced from the starting Mo^{VI} in MoS_4^{2-} to Mo^{IV} in the final product 2. The *cis–trans–cis* (with respect to sulfurs, pyridine and azo nitrogens respectively) configuration of the RuL_2S_2 fragment in 2 has been established by the ^{1}H NMR spectroscopy. In dichloromethane solution the complexes 2 exhibit a strong $d\pi(Ru^{II})\rightarrow L\pi^*$ MLCT transition near 550 nm, a strong sulfur to molybdenum LMCT transition near 500 nm and intra ligand $\pi-\pi^*$ transition in the UV region. In dichloromethane solution the complexes display reversible $Ru^{II}\rightleftharpoons Ru^{III}$ oxidation couples in the range 1.15–1.39 V, irreversible $Mo^{IV}\rightarrow Mo^{V}$ oxidations in the range 1.68–1.71 V vs SCE. Four successive reversible ligand (–N=N–) reductions are observed for each complex in the ranges $-0.37\rightarrow-0.67$ V (one-electron), $-0.81\rightarrow-1.02$ V (one-electron) and $-1.48\rightarrow-1.76$ V (simultaneous two-electron reduction) vs SCE respectively. The presence of trivalent ruthenium in the oxidized solutions 2^+ is evidenced by the rhombic EPR spectra. The EPR spectra of the coulometrically oxidized species 2^+ have been analyzed to furnish values of axial (Δ=4590–5132 cm^{-1}) and rhombic (ν=1776–2498 cm^{-1}) distortion parameters as well as energies of the two expected ligand field transitions (γ_1=3798–4022 cm^{-1}) and (γ_2=5752–6614 cm^{-1}) within the t_2 shell. One of the ligand field transitions has been observed experimentally at 6173 cm^{-1} and 6289 cm^{-1} for the complexes $2b^+$ and $2d^+$ respectively by near-IR spectra which are close to the computed γ_2 values.

Keywords: Ruthenium–molybdenum complexes; Sulfur bridging; Electron transfer

1. Introduction

There has been a continuous research activity in the area of transition metal complexes of tetrathiomolybdate ($Mo^{VI}S_4^{-2}$) anion. This is primarily due to its ability to form sulfur bridged heteronuclear complexes of the types $(L)M(\mu\text{-}S)_2MoS_2$, $S_2Mo(\mu\text{-}S)_2\text{-}M\text{-}(\mu\text{-}S)_2MoS_2$ and $(L)M(\mu\text{-}S)_2Mo(\mu\text{-}S)_2M(L)$ (M=Fe/Ru/Os) and moreover their relevance to the functional and structural models for the active sites of nitrogenase enzymes [1–12]. The present work originates from our interest to study the interaction of ruthenium azopyridine complexes $Ru^{II}(L)_2Cl_2$, 1, [L=2-arylazopyridine ligand, NC_5H_4N=NC_6H_5(R)] with the $Mo^{VI}S_4^{2-}$ unit. The reaction of 1 with the $(NH_4)_2MoS_4$ in 1:1 MeOH–H_2O medium unexpectedly results in a new class of sulfur bridged heteronuclear complexes of the type $(L)_2Ru^{II}(\mu\text{-}S)_2Mo^{IV}(OH)_2$ 2 where the terminal M^{VI}=S bonds of MoS_4^{2-} get hydroxylated with the concomitant 2-electron metal reduction, $Mo^{VI}\rightarrow Mo^{IV}$.

The MoS_4^{2-} unit is known to be sufficiently stable individually as well as on coordination and consequently the identity of MoS_4^{2-} has been retained in the earlier reported heteronuclear complexes [1–14]. However, the involvement of ruthenium–azopyridine moiety facilitates the hydroxylation of the terminal Mo=S bonds of MoS_4 in the complexes 2. To the best of our knowledge this work demonstrates the first example of internal transformation of MoS_4^{2-} unit on coordination. Herein we report the detailed synthetic account of the

formation of 2, the spectroscopic and electrochemical properties of the complexes 2.

2. Results and discussion

2.1. Synthesis

A group of five substituted arylazopyridine ligands (L^1–L^5) are used to prepare the ruthenium starting complexes, *ctc*-$Ru^{II}(L)_2Cl_2$ (1a–1e) (*ctc*=*cic*–*trans*–*cis* with respect to chlorides, pyridine and azo-nitrogens respectively). The reaction of complex 1 with the ammonium salt of tetrathiomolybdate (VI), $(NH_4)_2MoS_4$ in MeOH–H_2O (1:1) results in a dark-colored solid mass along with the deposition of elemental sulfur on the wall of the reaction flask. Chromatographic purification of the above crude product on a silica gel column using dichloromethane–acetonitrile (1:1) as eluent followed by removal of solvents under reduced pressure, affords a pure violet compound in the solid state having the composition $(L_2)Ru^{II}(\mu\text{-}S)_2Mo^{IV}(OH)_2$ (2) (Scheme 1). The formation of 2 (Scheme 1) is primarily involved with two simultaneously operating functions at the molybdenum center: (i) hydroxylation of Mo at the expense of Mo=S bond rapture and (ii) the reduction of Mo^{VI} in MoS_4^{2-} to Mo^{IV} in 2.

Since under similar reaction conditions (Scheme 1) but in the absence of 1 the MoS_4^{2-} unit remains unaffected, therefore it implies that the ruthenium fragment in 2 plays an important role to undergo the hydroxylation of the Mo=S bonds.

The *trans*–*cis* (with respect to pyridine and azo nitrogens respectively) configuration of the RuL_2 part of starting complexes 1 remain unaltered in the products 2 (see NMR part). The *ctc* isomer of the starting complexes RuL_2Cl_2, 1 is found to be thermodynamically most stable product and the other two isolated isomers of 1, *ttt* and *ccc* (*ttt*=*trans*–*trans*–*trans*; *ccc*=*cis*–*cis*–*cis* with respect to chlorides, pyridine and azo-nitrogens respectively) are known to be transformed into the most stable *ctc* isomer in only high boiling xylene and *N*,*N*-dimethylformamide solvents [15]. However, under identical reaction conditions (Scheme 1) the use of *ttt* or *ccc* isomer of 1 instead of *ctc* isomer results in only the product 2 where pyridine and azo-nitrogens of L are in the *trans* and *cis* configuration respectively. Since the identity of the *ttt* and *ccc* isomers of 1 remain intact in the boiling MeOH–H_2O medium, the formation of $Ru(\mu\text{-}S)_2Mo$ linkage in 2 might have forced the RuL_2 part of 2 to stabilize preferentially in the *trans*–*cis* configuration. Although the geometrical reorganization of the *ttt* isomer of 1 is essential to participate in the reaction as shown in Scheme 1, the conversion of the *cc* form of RuL_2 part to *tc* in 2 is not understandable particularly at the present mild reaction conditions (Scheme 1). We wish to note here that the reaction in Scheme 1 represents the first example where the *ttt* isomer of 1 has undergone the necessary geometrical reorientation to bind the incoming groups (here the bridging sulfurs) in the *cis* position whereas in earlier all cases *trans* chloride groups of the *ttt* isomer of 1 performed the chloride substitution reactions only at the trans position in presence of suitable monodentate ligands keeping the *tt* configuration of the RuL_2 part unchanged [16].

The microanalytical data of the products 2 (Table 1) are in very good agreement with the calculated values and thus confirm the composition. Solid state magnetic moment measurements at 298 K indicate that the complexes are uniformly diamagnetic, low-spin-Ru^{II}, t_{2g}^6, S=0; Mo^{+4} in a distorted tetrahedral arrangement setting the two metal electrons in the low-lying d_z^2 orbital in a paired configuration. In acetonitrile solution the complexes 2 behave as nonconducting [17,18].

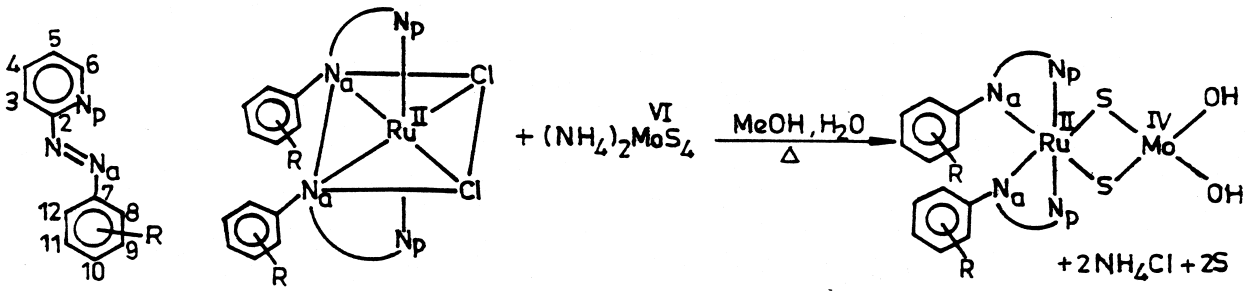

R = H	L^1	1a / 2a
R = 8-Me	L^2	1b / 2b
R = 8-Cl	L^3	1c / 2c
R = 9-Me	L^4	1d / 2d
R = 9-Cl	L^5	1e / 2e

Scheme 1.

Table 1
Microanalytical and electronic spectral data

Compd.	Elemental analysis (%)[a]			Electronic spectral data[b] λ_{max}(nm) (ϵ[c], M^{-1} cm^{-1})
	C	H	N	
2a	40.02 (39.93)	3.07 (3.02)	12.83 (12.70)	552(5398), 518[d](4507) 345(21557)
2b	41.86 (41.79)	3.39 (3.48)	12.27 (12.19)	549(4479), 515[d](4070), 319(13600)
2c	36.28 (36.16)	2.57 (2.46)	11.43 (11.50)	558(4343), 507[d](3100), 314(14030)
2d	41.71 (41.79)	3.42 (3.48)	12.28 (12.19)	546(7826), 500[d](5708), 346(31337)
2e	36.25 (36.16)	2.53 (2.46)	11.59 (11.50)	563(3409), 509[d](2777), 332(13866)

[a] Calculated values are in paranthesis.
[b] In dichloromethane.
[c] Extinction coefficient.
[d] Shoulder.

2.2. Thermal analysis

Thermogravimetric analysis (TGA) of the complexes 2 show a three-step decomposition pattern. The three successive decompositions take place near 250°, 340° and 375°C corresponding to the weight loss of one water molecule, two sulfur atoms and the two ligands (L) respectively. The differential thermal analysis of complexes 2 further confirm the above decomposition pattern. It shows one broad endothermic peak at 250°C due to removal of water followed by another endotherm near 350°C for the elimination of sulfur and a large exothermic peak near 380°C indicating the loss of ligand (L) molecules.

2.3. Spectral study

2.3.1. Infrared spectra

The IR spectra of the complexes (2) were recorded as KBr discs in the range 4000–400 cm^{-1}. Two important features are: (i) complexes exhibit a moderately strong and broad band near 3400 cm^{-1} due to OH stretching frequency [19] and (ii) a strong band near 1350 cm^{-1} due to coordinated azo (–N=N–) stretching frequency. In order to confirm the origin of the 3400 cm^{-1} band the IR spectrum of blank KBr pellet was recorded. Since the blank KBr pellet did not show any band in the range 4000–400 cm^{-1}, it can therefore be inferred that the observed band at 3400 cm^{-1} is developed certainly due to the presence of Mo–OH bonds in the complexes (2). The ν(N=N) of the free ligand (L) appears near 1425 cm^{-1} which has been shifted to 1350 cm^{-1} on coordination in the complexes 2 due to strong $d\pi(Ru^{II})\rightarrow\pi^*$(L) back-bonding in the ground state of ruthenium(II) where π^* (L) is primarily dominated by the –N=N– function [20].

2.3.2. FAB mass spectrum

FAB mass spectrum of one representative complex (2a) was recorded and the spectrum is shown in Fig. 1. The maximum molecular peak is observed at m/z, 662 which corresponds to the molecular ion $[(NC_5H_4N{=}NC_6H_5)_2Ru^{II}(\mu\text{-}S)_2Mo^{IV}(OH)_2]$, (calculated molecular weight 661.6). A careful examination of the fragmentation pattern of the FAB mass spectrum of 2a reveals the stepwise eliminations of H_2O, MoO, 2S, Ru/L and L fractions.

2.3.3. ^1H NMR spectra

The complexes display well resolved ^1H NMR spectra in DMSO-d^6 solvent. Chemical shift and spin–spin splitting among nearest neighbor protons are depicted in Table 2. One representative spectrum is shown in Fig. 2. The presence of C_2 symmetry makes each half of the molecule equivalent. Thus one methyl signal has been observed for the complexes 2b and 2d. Similarly aromatic region of the spectra exhibit calculated number of protons correspond to one particular ligand in accord with the symmetry. The individual aromatic proton resonances are assigned on the basis of their relative intensities, spin-spin structure and substituent induced splitting patterns [21,22]. Chemical shifts are also considered as additional indicators such as 8-H and 12-H are coincident-doublets in complex 2a whereas 8-H signal appears as a singlet for the complexes 2d and 2e. Further, the 8-H singlet is significantly shifted to higher and lower fields in the complexes 2d and 2e respectively compared to 2a (Table 2) based on the electron releasing and withdrawing properties of the methyl and chloride substituents respectively. Similarly the *ortho* substituted complexes (2b, 2c) show the expected changes in the distributions of the phenyl ring proton signals.

The chemical shift of the methyl group follows the

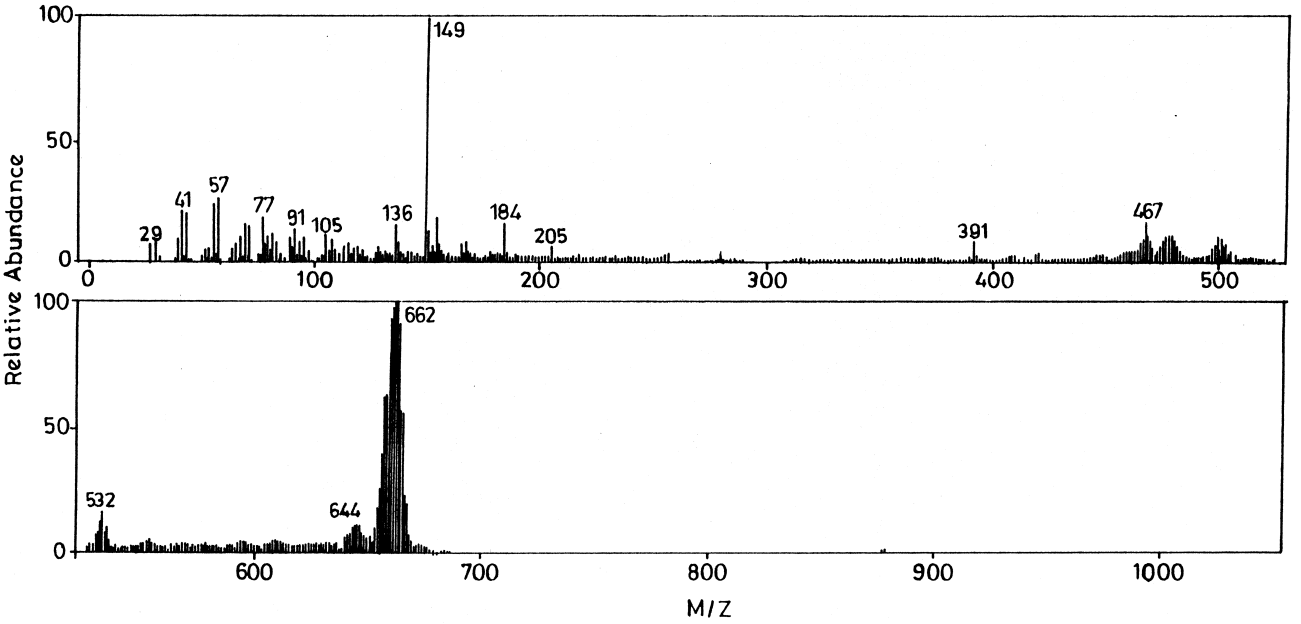

Fig. 1. FAB mass spectrum of $[(L^1)_2Ru^{II}(\mu\text{-}S)_2Mo^{IV}(OH)_2]$, 2a.

order: *o*-Me (2b), 2.5ppm>*m*-Me (2d), 2.18 ppm, indicating the effect of nearby electron withdrawing azo group on the *ortho* methyl group is more as compared to the meta methyl group as expected [23].

Although we were unable to grow suitable single crystals for X-ray characterization, the FAB mass, infrared, ^{1}H NMR spectroscopic results along with the thermal analysis, microanalytical, conductivity, magnetic moment data collectively establish the composition and stereochemistry of the complexes 2.

2.3.4. Electronic spectra

The electronic spectra of the complexes (2) were studied in dichloromethane solvent in the region 200–900 nm. The spectral data are listed in Table 1 and one representative spectrum is shown in Fig. 3. In the visible region the complexes display one moderately intense band near 550 nm associated with a shoulder at the higher energy part near 500 nm. On the basis of their high intensities these two bands are assigned as charge-transfer in nature. The lowest energy band near 550 nm is assigned to be

Table 2
^{1}H NMR spectral data in $(CD_3)_2SO$

δ(J/Hz)[a]									
Compd.	3H	4H	5H	6H	8H	9H	10H	11H	12H
2a	8.62 (8.37)[b]	8.12 (7.67)[c] (8.09)	7.69 (6.42)[c] (6.79)	8.82 (5.70)[b]	7.19 (8.37)[b]	7.30 (7.67)[c] (7.67)	7.43 (6.67)[c] (6.97)	7.30 (7.67)[c] (7.67)	7.19 (8.37)[c]
2b	8.47 (8.10)[b]	8.03 (7.37)[c] (7.31)	7.86 (8.10)[c] (7.97)	8.91 (5.53)[b]	Me (2.50)	6.15 (8.10)[b]	7.14 (7.37)[c] (7.73)	6.70 (7.74)[c] (7.37)	7.24 (8.8)[b]
2c	8.45 (7.85)[b]	7.98 (7.81)[c] (8.12)	7.67 (8.01)[c] (7.82)	8.98 (5.49)[b]	(Cl)	6.82 (7.90)[b]	7.04 (7.20)[c] (7.51)	7.17 (7.82)[c] (7.42)	7.21 (7.90)[b]
2d	8.63 (8.15)[b]	8.15 (7.83)[c] (8.15)	7.72 (6.45)[c] (6.80)	8.84 (5.10)[b]	6.89[d]	(Me) (2.18)	6.99 (7.50)[b]	7.20 (8.1)[c] (8.5)	7.25 (8.5)[b]
2e	8.40 (7.55)[b]	7.90 (7.91)[c] (8.27)	7.62 (7.19)[c] (7.92)	9.18 (5.39)[b]	7.16[d]	(Cl)	7.10 (8.27)[b]	7.48 (7.19)[c] (7.19)	7.54 (8.4)[d]

[a] Tetramethylsilane as internal standard.
[b] Doublet.
[c] Triplet.
[d] Singlet.

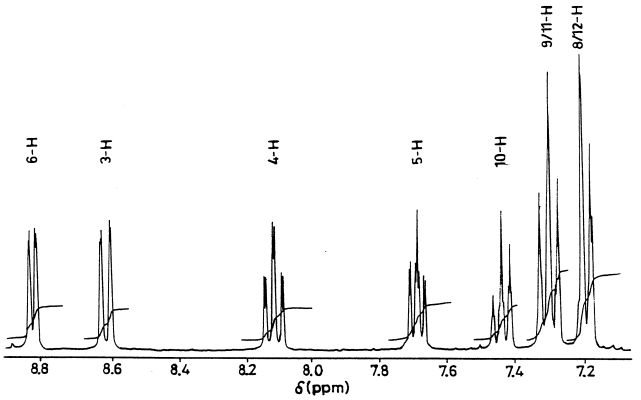

Fig. 2. ^{1}H NMR spectrum of $[(L^1)_2Ru^{II}(\mu\text{-}S)_2Mo^{IV}(OH)_2]$, 2a in DMSO-$d^6$.

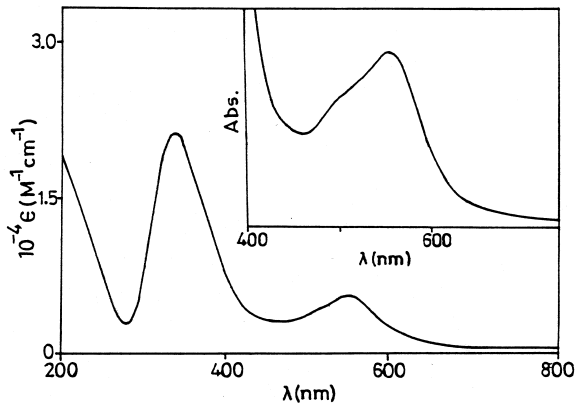

Fig. 3. Electronic spectrum of $[(L^1)_2Ru^{II}(\mu\text{-}S)_2Mo^{IV}(OH)_2]$, 2a in dichloromethane at 298 K. The inset shows an expansion of the MLCT bands.

$d\pi(Ru^{II})\rightarrow\pi^*(L)$ MLCT transition where $\pi^*(L)$ is believed to be primarily dominated by the LUMO of the azoimine chromophore [20]. For the starting complexes 1 the $d\pi(Ru^{II})\rightarrow\pi^*(L)$ MLCT transition occurs near 580 nm [20]. The charge-transfer transition energy is known to depend on the separation in potentials between the donor and acceptor levels [24–26]. In the complexes 2 the difference in potentials between the first reduction couple (–N=N– reduction) and the reversible oxidation couple (Ru^{II}–Ru^{III}) is ~1.8 V (Table 3) which is higher than that of the starting complexes 1 (~1.6 V) [20]. In view of the above observation it may be considered that the MLCT transition which occurs at 580 nm for the starting complexes 1 has been shifted to 550 nm in the complexes 2. This increase in MLCT transition energy on moving from 1 to 2 implies that the filled ruthenium t_{2g} level becomes stabilized further in the present ligand environments compared to those of 1. The higher energy shoulder near 500 nm may be assigned to the charge-transfer transition from sulfur to molybdenum since a similar strong sulfur to molybdenum charge-transfer transition has been observed in the range 400–500 nm for various cluster compounds involving MoS_4 moiety [27–29]. In the UV region the complexes show one intense transition near 350 nm possibly due to intraligand $\pi-\pi^*$ transition involving energy level higher than that of the ligand LUMO [20].

2.4. Electron-transfer properties

The electron-transfer properties of the complexes (2) were studied by cyclic voltammetry in dichloromethane solvent vs a saturated calomel electrode (SCE) using platinum working electrode. Representative voltammo-

Table 3
Electrochemical data at 298 K[a]

Compd.	Ru^{III}–Ru^{II} couple E^0_{298}/V (ΔE_p/mV)	$Mo^{IV}\rightarrow Mo^V$ oxidation, E_{pa}[b]/V	Ligand reductions E^0_{298}/V (ΔE_p/mV)	ΔE^0/V[c]	γ_{MLCT}/cm^{-1}	
					Cal.[d]	Obs.[e]
2a	1.30 (100)	1.70	−0.50(100), −0.92(110), −1.65(120)	1.80	17517	18115
2b	1.15 (110)	1.71	−0.67(100), −1.02(120), −1.76(120)	1.82	17678	18215
2c	1.39 (100)	1.69	−0.37(90), −0.81(100), −1.48(120)	1.76	17194	17921
2d	1.24 (90)	1.68	−0.60(100), −0.96(110), −1.69(110)	1.84	17840	18315
2e	1.35 (120)	1.69	−0.42(100), −0.86(110), −1.54(120)	1.77	17275	17762

[a] Condition: solvent, dichloromethane; supporting electrolyte, TBAP; reference electrode, SCE; solute concentration, ~10^{-3} M; working electrode, platinum wire.
[b] E_{pa} is considered due to irreversible nature of the voltammograms.
[c] Calculated by using Eq. (7) from the text.
[d] Using Eq. (6) from the text.
[e] In CH_2Cl_2 solution.

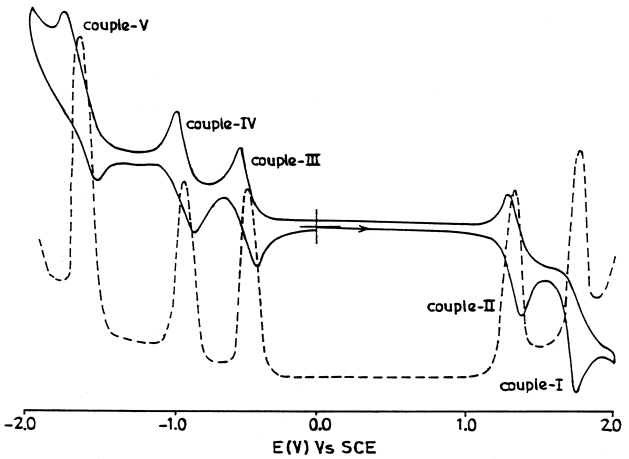

Fig. 4. Cyclic voltammograms and differential pulse voltammograms of ~10^{-3} M solution of $[(L^1)_2Ru^{II}(\mu\text{-}S)_2Mo^{IV}(OH)_2]$, 2a in dichloromethane at 298 K.

grams are shown in Fig. 4 and the reduction potentials data are listed in Table 3. The complexes are electroactive with respect to the metal as well as ligand centers and display the same five redox processes (couples I–V) in the potential range ±2 V vs SCE. The assignments of the responses to specific couples are based on the following considerations.

2.4.1. The ruthenium(III)–ruthenium(II) couple

The complexes display one quasi-reversible oxidative response in the region 1.15–1.39 V (couple-II, Fig. 4). The one-electron nature of the couple-II was confirmed by constant-potential coulometry (see later). This process is assigned to the oxidation of the starting bivalent ruthenium(II) species to the trivalent ruthenium(III) congener, Eq. (1). The presence of the trivalent-ruthenium in the oxidized solution was confirmed by the characteristic rhombic EPR spectrum

$$[(L)_2Ru^{III}(\mu\text{-}S)_2Mo^{IV}(OH)_2]^{2+} + e^- \rightleftharpoons [(L)_2Ru^{II}(\mu\text{-}S)_2Mo^{IV}(OH)_2] \quad (1)$$

of the low-spin ruthenium(III) complex (Fig. 5a) [30–33]. The formal potential of the couple (Eq. (1)) varies depending on the nature of the R group present in the ligand (L) as expected [34] (Table 3).The ruthenium(III)–ruthenium(II) potential of the starting complexes 1 appears in the range 1.02–1.30 V vs SCE [20]. Thus formation of the sulfur bridged ruthenium–molybdenum dimer in 2 increases the Ru^{II}–Ru^{III} oxidation potential by 100–150 mV.

2.4.2. The molybdenum(IV)–molybdenum(V) oxidation

The complexes 2 exhibit a second irreversible oxidation process near 1.7 V (anodic peak, E_{pa}) vs SCE (couple I, Fig. 4). No significant response on scan reversal in cyclic voltammetry is observed (Fig. 4, Table 3). The oxidized

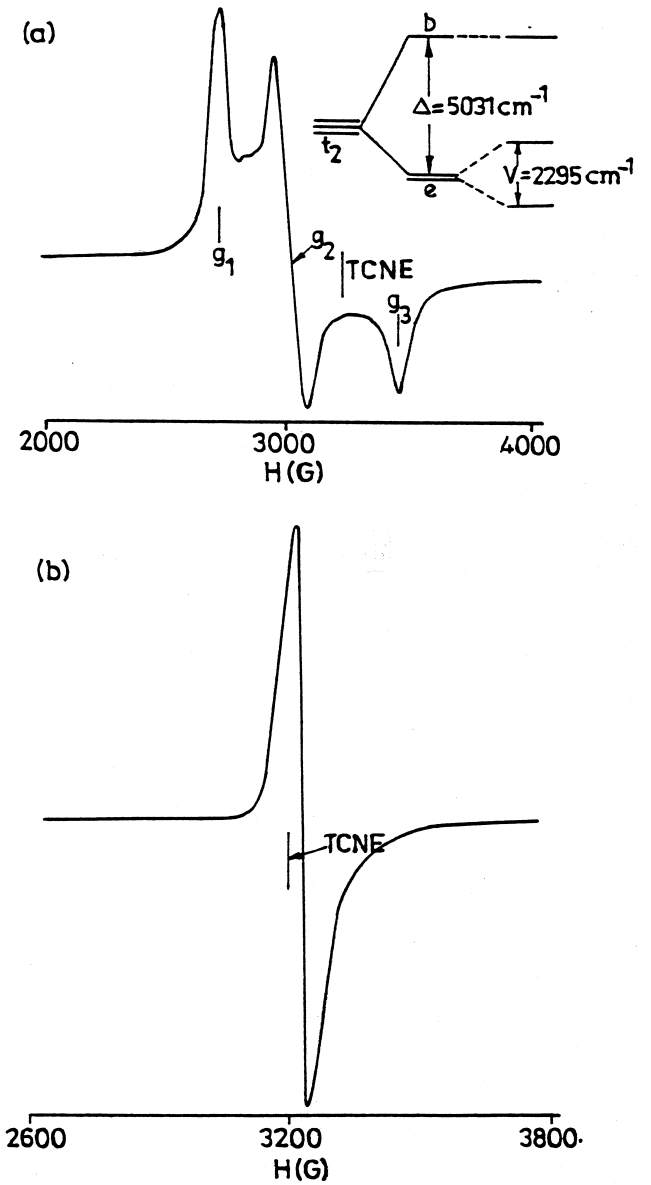

Fig. 5. (a) X-band EPR spectrum and computed t_2 splitting of the coulometrically oxidized complex $[(L^2)_2Ru^{III}(\mu\text{-}S)_2Mo^{IV}(OH)_2]^+$, $2b^+$ in dichioromethane at 77 K. (b) X-band EPR spectrum of the coulometrically reduced complex $[(L^3)_2Ru^{II}(\mu\text{-}S)_2Mo^{IV}(OH)_2]^-$, $2c^-$ in dichloromethane solution at 77 K.

species thus decomposes rapidly on cyclic voltammetric time scale. Although the anodic current height (i_{pa}) of this irreversible process is ~1.5 times greater than that of the previous reversible ruthenium(II)–ruthenium(III) process, the differential pulse voltammogram shows the second oxidation wave to have the same current height as that of the first, implying a one-electron process (Fig. 4). This irreversible oxidation process could be due to either $Ru^{III} \rightarrow Ru^{IV}$ oxidation or oxidation of the molybdenum(IV) to molybdenum(V). Here the potential difference between the two successive oxidation processes is ~0.4 V. The average potential differences between the two successive redox processes of the ruthenium center ($Ru^{II/III}$–$Ru^{III/IV}$) in mononuclear complexes having C, N,

O, thioether donor centers have been observed in many cases to be in the range 1.3–1.5 V [19,30–33,35–37]. Therefore it seems reasonable to consider this irreversible response as due to oxidation of the Mo^{IV}–Mo^{V} center.

2.4.3. Ligand reduction

The complexes 2 display three successive reductions (couples III–V, Fig. 4) at the negative side of SCE. The one-electron stoichiometry of couples III and IV and two-electron stoichiometry of couple V are identified by comparison with the ruthenium(III)–ruthenium(II) couple (couple II) with the help of cyclic voltammetric current height as well as differential pulse voltammetry (Fig. 4). The ligand L is known to act as a potential electron-transfer center [38]. Each ligand can accept two electrons in the electrochemically accessible LUMO which is predominantly azo in character. As two electroactive azo groups are present in the complexes 2, four successive one-electron reductions are expected for each complex (Eqs. (2)–(5)).

$$[Ru^{II}L_2(\mu-S)_2Mo^{IV}(OH)_2] + e^- \rightleftharpoons [Ru^{II}L(L^{\bullet-})(\mu-S)_2Mo^{IV}(OH)_2]^- \quad (2)$$

$$[Ru^{II}L(L^{\bullet-})(\mu-S)_2Mo^{IV}(OH)_2]^- + e^- \rightleftharpoons [Ru^{II}(L^{\bullet-})_2(\mu-S)_2Mo^{IV}(OH)_2]^{2-} \quad (3)$$

$$[Ru^{II}(L^{\bullet-})_2(\mu-S)_2Mo^{IV}(OH)_2]^{2-} + e^- \rightleftharpoons [Ru^{II}(L^{\bullet-})(L^{2\bullet-})(\mu-S)_2Mo^{IV}(OH)_2]^{3-} \quad (4)$$

$$[Ru^{II}(L^{\bullet-})(L^{2\bullet-})(\mu-S)_2Mo^{IV}(OH)_2]^{3-} + e^- \rightleftharpoons [Ru^{II}(L^{2\bullet-})_2(\mu-S)_2Mo^{IV}(OH)_2]^{4-} \quad (5)$$

In practice all the four reductions [Eqs. (2)–(5)] are observed experimentally. Instead of observing all the four-ligand based reductions separately, the first two reductions [Eqs. (2) and (3)] appear distinctly (couples III and IV), the other two reductions [Eqs. (4)–(5)] being overlapped (couple V, Fig. 4) [15,34].

2.4.4. Electrogeneration of the oxidized (2^+) and reduced (2^-) species

Coulometric oxidations of the complexes 2 in dichloromethane solution at a potential 100 mV positive to the corresponding E_{pa} of Ru^{II}/Ru^{III} couple (couple II, Fig. 4) at 298 K produce unstable oxidized species. However, at 268 K coulometric oxidation of 2 generates a green solution and the observed Coulomb count corresponds to one-electron transfer (''*n*'' values: 2a, 0.98; 2b, 0.97; 2c, 1.04; 2d, 0.95, 2e, 1.07; $n = Q/Q'$ where Q' is the calculated Coulomb count for a one-electron transfer and Q is that found after exhaustive electrolysis of 10^{-2} mmol of solute). The resulting oxidized solutions ($2a^+$–$2e^+$) display voltammograms which are superposable on those of the corresponding bivalent complexes (2a–2e) which imply that the oxidations here may be stereoretentive in nature [39]. When the same green oxidized solutions were coulometrically reduced at 0.7 V vs SCE the parent bivalent Ru(II) congeners 2 were formed quantitatively. The X-band EPR spectra of the freshly prepared oxidized solutions (produced coulometrically at 268 K followed by quick freezing in liquid N_2, 77 K) were examined. The oxidized complexes 2^+ display rhombic EPR spectra (Fig. 5a, Table 4). The rhombic nature of the EPR spectra are characteristic of low-spin trivalent ruthenium(III) complexes (low-spin, t_{2g}^5, $S = 1/2$) in a distorted octahedral environment [30–33]. The reactive nature of the oxidized species (2^+) at room-temperature has precluded its isolation in the solid state.

The theory of EPR spectra of low-spin d^5 complexes are documented in literature [40–46]. The distortion of pseudo octahedral complexes is expressed as the sum of axial (Δ) and rhombic (V) components. The t_2 orbital consists of the components $t_2^0(xy)$, $t_2^+(xz)$, $t_2^-(yz)$. The degeneracy of t_2 orbital is partially removed by axial distortion (Δ), which placed t_2^0 (b) above t_2^+/t_2^- (e). The superimposed (V) then further splits (e) into t_2^+ and t_2^-.

The distortion parameters (Δ and V) and the energies of two optical transitions (v_1 and v_2) from ground to upper Kramers doublets can be obtained from the analysis of EPR spectra using the g tensor theory of low-spin d^5 ions [40–46].

The EPR spectra provide only the absolute g values and so neither their signs nor the correspondence of g_1, g_2 and g_3 to g_x, g_y and g_z are known. There are forty-eight possible combinations based on the labeling (x,y,z) and signs chosen for the experimentally observed g values. For the present case we have chosen the combination $-g_1 > -g_2 > g_3$ as this particular set gives the orbital reduction

Table 4
EPR g values[a] and distortion parameters[b]

Compound	g_1	g_2	g_3	k	Δ/λ	V/λ	v_1/λ	v_2/λ	v_2/λ (obs.)
2a	−2.34	−2.17	1.86	0.71	5.13	−2.49	3.98	6.61	–
2b	−2.34	−2.17	1.86	0.70	5.03	−2.29	3.98	6.42	6.17
2c	−2.33	−2.18	1.84	0.66	4.59	−1.76	3.79	5.75	–
2d	−2.34	−2.17	1.86	0.70	5.05	−2.26	4.02	6.43	6.28
2e	−2.33	−2.18	1.85	0.68	4.76	−1.97	3.87	6.01	–

[a] In dichloromethane solution at 77 K.
[b] Meanings are given in the text.

factor, $k<1.0$ The computed values of orbital reduction factor (k), axial distortion (Δ/λ), rhombic distortion (V/λ) and the two ligand–field optical transitions (v_1/λ and v_2/λ) for the complexes 2^+ are listed in Table 4. The value of spin–orbit coupling constant (λ) of ruthenium(III) is taken as 1000 cm^{-1} [40–46]. Here axial distortion is found to be two times greater than that of the rhombic component.

We have been succeeded to record the low energy near-IR spectra (maximum wavelength scan up to 2200 nm) of two complexes $2b^+$ and $2d^+$ and they display one weak transition at 1620 nm (ϵ, $M^{-1}cm^{-1}$, 45) and 1590 nm (ϵ, $M^{-1}cm^{-1}$, 60) respectively (Table 4). In view of the involved approximations in the theory, the agreement between the experimentally observed v_2 and calculated v_2 value is excellent (Table 4). Due to instrumental limitation (maximum wavelength scan up to 2200 nm) it has not been possible to compare the v_1 band.

The coulometrically produced reduced brown solutions [obtained by reducing the complexes 2 at a potential 100 mV negative to the corresponding E_{pc} of couple III (Fig. 4)] are unstable even at 268 K. However, we have managed to record the EPR spectrum of the reduced complex $2c^-$ by performing the electrolysis at 258 K (observed Coulomb count corresponds to one-electron transfer, $n=1.09$ and the reduced brown solution exhibits voltammograms which are superposable on those of the parent complex) and quickly freezing the electrolyzed solution (liquid nitrogen, 77 K). The reduced solution $2c^-$ shows an intense, symmetric and sharp EPR signal with ''g'' value at 1.997 as shown in Fig. 5b. This suggests that the unpaired electron in the reduced product (2^-) is localized in the orbital of predominantly ligand character [39]. This provides strong support in favor of the successive addition of electrons to the azo functions of the ligands L as proposed in the previous ligand reduction part. Coulometric reductions of the couples IV and V (Fig. 4) generated the unstable reduced species even at 258 K.

2.4.5. Spectroelectrochemical correlation

Complexes (2) display lowest MLCT transition of the type $t_2(Ru^{II})\rightarrow$Ligand LUMO (where the LUMO is dominated by the azo function of L) near 550 nm (Table 1, Fig. 3). The quasi-reversible ruthenium(III)–ruthenium(II) reduction potentials in the range 1.15–1.39 V and the first ligand (–N=N–) reduction potentials in the range $-0.3\rightarrow-0.5$ V (Table 3). Here the MLCT transition involves excitation of the electron form the filled t_{2g}^6 orbital of ruthenium(II) to the lowest π^* orbital of the azo function of L. The energy of this band can be predicted from the experimentally observed electrochemical data with the help of Eq. (6) and (7) [47]. Here E^0_{298} (Ru^{III}–Ru^{II}) is the formal potential (in V) of the quasi-reversible ruthenium(III)–ruthenium(II) couple, E^0_{298}(L) that of the first ligand

$$\nu_{MLCT} = 8065(\Delta E^0) + 3000 \quad (6)$$

$$\Delta E^0 = E^0_{298}(Ru^{III} - Ru^{II}) - E^0_{298}(L) \quad (7)$$

reduction and ν_{MLCT} is the frequency or energy of the charge-transfer band in cm^{-1}. The factor 8065 is used to convert the potential difference ΔE from V into cm^{-1} unit and the term 3000 cm^{-1} is of empirical origin. The calculated and experimentally observed ν_{MLCT} transitions are listed in Table 3 and there is a linear relationship between the γ_{MLCT} and ΔE (Fig. 6). Here the calculated values for all the complexes lie within 800 cm^{-1} of the experimentally observed charge-transfer energies, which are in good agreement with the observations of previous workers on other ruthenium complexes [48–51].

The formation of complex 2 starting from 1 and MoS_4^{2-} in aqueous methanol medium is complex in nature as the formation 2 is associated with simultaneously operating substitution, elimination and electron-transfer processes at the molybdenum center. However, the following tentative rationale (Scheme 2) may be proposed. Since the formation of elemental sulfur from each Mo=S bond involve 2-electrons oxidation, therefore the generation of total four electrons due to the cleavage of two Mo=S bonds possibly reduce the molybdenum from +6 oxidation state to +2 oxidation state followed by aquation in presence of water as the first step of the reaction (A, Scheme 2). This may account for the need of water in the reaction medium (Scheme 1). As the +2 oxidation state of molybdenum is known to be highly reducing in character [52], it is therefore subsequently oxidized to Mo^{IV} via the reduction of H^+ ions (formed by the autoionization of H_2O) of the coordinated H_2O molecules (A, Scheme 2) to H_2. All the consecutive processes in Scheme 2 may lead to the formation of 2 as a final product.

The role of the ruthenium azopyridine moiety on the hydroxylation of the Mo=S bonds in 2 is not clear, however, the strong π-acidic nature of L and consequently its inherent tendency to stabilize the lower oxidation states of the metal ions [53] might have played an important role to carry out the reaction in Scheme 1.

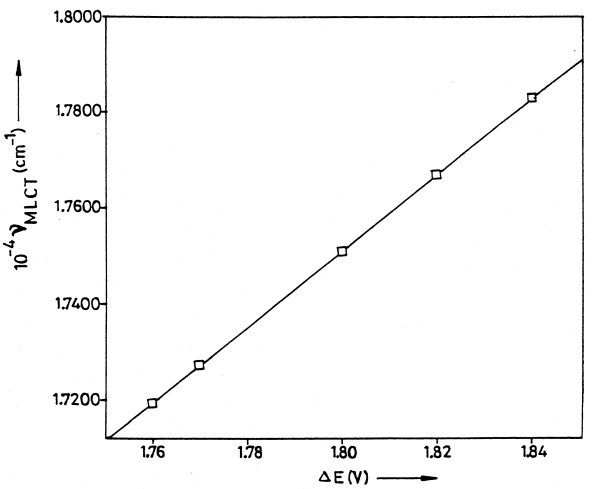

Fig. 6. Least squares plot of the lowest energy metal-to-ligand charge-transfer band (ν_{MLCT}, cm^{-1}) vs the difference in potential (ΔE, V) between the $Ru^{II/III}$ couple and the first ligand reduction.

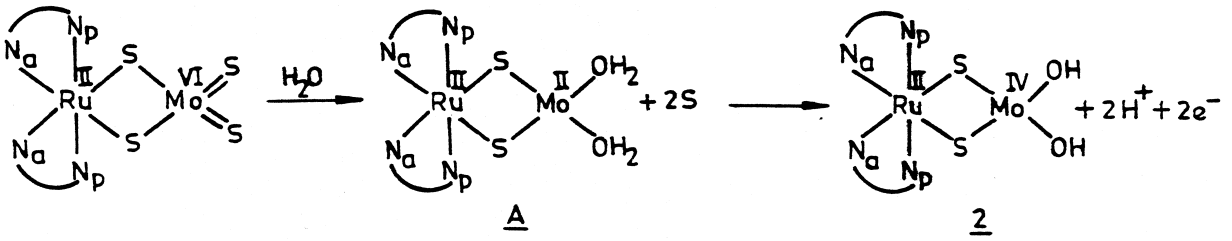

Scheme 2.

3. Conclusions

We have observed a new class of sulfur bridged ruthenium–molybdenum dinuclear species (2) where the terminal Mo=S bonds of the well known stable $Mo^{VI}S_4^{2-}$ unit have been hydroxylated with the concomitant two-electrons reduction at the molybdenum center. The formation of Ru(μ-S)$_2$Mo linkage stabilizes the RuL_2 fragment of 2 preferentially in the *trans–cis* configuration (*trans–cis* with respect to pyridine and azo nitrogens of L). The complexes 2 display successive metal and ligand based electron-transfer processes.

The complexes 2 can act as a stepping stone for the formation of mixed sulfur and hydroxo bridged as well as sulfur and oxo bridged complexes of type M(μ-S)$_2$Mo(μ-OH)$_2$M′ and M(μ-S)$_2$Mo(μ-O)$_2$M′, where M=M′=Ru or M=Ru, M′=Os. Works are in progress in this direction.

4. Experimental

4.1. Materials

Commercial ruthenium trichloride (S.D. Fine Chemicals, Bombay, India) was converted into $RuCl_3.3H_2O$ by repeated evaporation to dryness with concentrated hydrochloric acid. The ligands L, starting metal complexes $[RuL_2Cl_2]$ [23] and $(NH_4)_2MoS_4$ [54] were prepared according to the reported procedures. Other chemicals and solvents were reagent grade and used as received. Silica gel (60–120 mesh) used for chromatography were of BDH quality. For spectroscopic/electrochemical studies HPLC grade solvents were used. Commercial tetrabutylammonium bromide was converted into pure tetrabutylammonium perchlorate by following an available procedure [55].

4.2. Physical measurements

Solution electrical conductivity was checked using Systronic 305 conductivity bridge. Electronic spectra (900–200 nm) were recorded using a Shimadzu-UV 160 A spectrophotometer, IR spectra on a Nicolet FT-spectrophotometer with samples prepared as KBr pellets. Magnetic susceptibility was checked with a PAR vibrating sample magnetometer.

Proton NMR spectra were obtained with a 300 MHz Varian FT–NMR spectrometer. Cyclic voltammetric measurements were carried out using a PAR model 373 A potentiostat–galvanostat electrochemistry system. A platinum-wire working electrode, a platinum-wire auxiliary electrode and an aqueous saturated calomel reference electrode were used in a three-electrode configuration. The supporting electrolyte was NBu_4ClO_4 and the solute concentration $\approx 10^{-3}$ M. The half-wave potential E^0_{298} was set equal to 0.5 ($E_{pa}+E_{pc}$), where E_{pa} and E_{pc} are the anodic and cathodic cyclic voltammetric peak potentials respectively. The scan rate was 50 mVs^{-1}. The coulometric experiments were done with a PAR model 373 A electrochemistry system. A platinum wire-gauze working electrode was used in coulometric experiments. All electrochemical experiments were carried out under a dinitrogen atmosphere. All electrochemical data were collected at 298 K and are uncorrected for junction potential. The EPR measurements were made with a Varian model 109 C E-line X-band spectrometer fitted with a quartz Dewar for measurements at 77 K (liquid nitrogen). The spectrum was calibrated by using tetracyanoethylene (TCNE) (g= 2.0037). The elemental analyses were carried out with a Carlo Erba (Italy) elemental analyzer. The TGA and DTA experiments were performed by using a Dupont 9900 instrument. FAB mass spectrum at 298 was recorded on a SX 102/DA-6000 mass spectrometer.

4.3. Treatment of EPR data

An outline of the procedure can be found in our recent publications [40–46,56,57]. We would like to note that a second solution also exists that is also different from the chosen one, having small Δ, V, v_1 and v_2 values. The experimentally observed near-IR results clearly eliminate this solution as acceptable.

4.4. Preparation of complexes

The complexes (2a–2e) were prepared by using a general procedure. Yield varies in the range 60–65 %. Specific details are given for one representative complex (2a).

The starting complex *ctc*-RuL_2Cl_2, 1a (100 mg, 0.19 mmol) and $(NH_4)_2MoS_4$ (48 mg, 0.19 mmol) were dissolved separately in MeOH (20 ml) and H_2O (20 ml) respectively. The aqueous solution of $(NH_4)_2MoS_4$ was added to the warm methanolic solution of 1a and the

resulting mixture was heated to reflux for overnight and then cooled. A dark colored solid product separated which was collected by filtration, washed thoroughly with water and methanol and finally dried in vacuo over P_4O_{10}. The dried product was dissolved in minimum volume of dichloromethane and purified by using a silica gel column (60–120 mesh). Using dichloromethane–acetonitrile (1:1) as eluent a red violet band was eluted leaving behind a dark band at top of the column. The violet fraction was collected and evaporation of the solvents under reduced pressure afforded solid compound 2a. Finally the product was recrystallized from dichloromethane–hexane (1:4). Yield: 63%.

Acknowledgements

Financial support received from the Department of Science and Technology, New Delhi, India, is gratefully acknowledged. Special acknowledgements are made to the Regional Sophisticated Instrumentation Center (RSIC), I.I.T., Bombay, for providing NMR and EPR facilities and RSIC, Central Drug Research Institute, Lucknow, for providing FAB Mass spectrum. The referees comments at the revision stage were very helpful.

References

[1] G.A. Bowmarker, P.W.D. Boyd, R.J. Sorrensen, C.A. Read, J.W. McDonald, Inorg. Chem. 24 (1985) 3.
[2] K.P. Callahan, P.A. Piliero, Inorg. Chem. 19 (1980) 2619.
[3] P. Stremple, N.C. Baenziger, D. Coucouvanis, J. Am. Chem. Soc. 103 (1981) 4601.
[4] D. Coucouvanis, A. Hadjikyriacou, Inorg. Chem. 26 (1987) 1.
[5] Y. Do, E.D. Simhon, R.H. Holm, Inorg. Chem. 24 (1985) 4635.
[6] J.M. Charnock, S. Bristow, J.R. Nicholson, C.D. Garner, W. Clegg, J. Chem. Soc., Dalton Trans. (1987) 303.
[7] E.M. Kinsch, D.W. Stephan, Inorg. Chim. Acta. 96 (1985) L87.
[8] J.M. Manoli, C. Potvin, F. Secheresse, S. Marzak, J. Chem. Soc., Chem. Commun. (1986) 1557.
[9] K.E. Howard, T.B. Rauchfuss, S.R. Wilson, Inorg. Chem. 27 (1988) 1710.
[10] M.A. Greaney, C.L. Coyle, M.A. Harmer, A. Jordan, E.I. Stiefel, Inorg. Chem. 28 (1989) 912.
[11] M. Karo, M. Kawano, H. Taniguchi, M. Funaki, H. Moriyama, T. Sato, K. Matsumoto, Inorg. Chem. 31 (1992) 26.
[12] R.H. Tieckelmann, H.C. Silvis, T.A. Kent, B.H. Huynh, J.V. Waszczak, B.K. Teo, B.A. Averill, J. Am. Chem. Soc. 102 (1980) 5550.
[13] W.H. Pan, M.E. Leonowicz, E.I. Stiefel, Inorg. Chem. 22 (1983) 672.
[14] E. Diemann, A. Muller, Coord. Chem. Rev. 10 (1973) 79.
[15] B.K. Santra, G.K. Lahiri, J. Chem. Soc., Dalton Trans., (1997) 129.
[16] S. Goswami, A.R. Chakravarty, A. Chakravorty, Inorg. Chem. 21 (1982) 2737.
[17] B.K. Santra, G.A. Thakur, P. Ghosh, A. Pramanik, G.K. Lahiri, Inorg. Chem. 35 (1996) 3550.
[18] E.I. Stiefel, Prog. Inorg. Chem. 22 (1977) 100.
[19] G.K. Lahiri, S. Bhattacharya, M. Mukherjee, A.K. Mukherjee, A. Chakravorty, Inorg. Chem. 26 (1987) 3359.
[20] S. Goswami, A.R. Chakravarty, A. Chakravorty, Inorg. Chem. 20 (1981) 2246.
[21] G.K. Lahiri, S. Goswami, L.R. Falvello, A. Chakravorty, Inorg. Chem. 26 (1987) 3365.
[22] B. Pesce, in: Nuclear Magnetic Resonance in Chemistry, Academic Press, New York, 1965, p. 174.
[23] P. Munshi, R. Samanta, G.K. Lahiri, Polyhedron 17 (1998) 1913.
[24] E.S. Dodsworth, A.B.P. Lever, Chem. Phys. Lett. 119 (1985) 61.
[25] N. Bag, A. Pramanik, G.K. Lahiri, A. Chakravorty, Inorg. Chem. 31 (1992) 40.
[26] P. Ghosh, A. Chakravorty, Inorg. Chem. 23 (1984) 2242.
[27] K. Tanaka, M. Morimoto, T. Tanaka, Inorg. Chim. Acta. 56 (1981) L61.
[28] E. Diemann, A. Muller, Coord. Chem. Rev. 10 (1973) 79.
[29] R.H. Tieckelman, H.C. Silvis, J.A. Kerit, B.H. Huynh, J.V. Waszczak, B.K. Teo, B.A. Verill, J. Am. Chem. Soc. 102 (1980) 5550.
[30] B.M. Holligam, J.C. Jeffery, M.K. Norgett, E. Schatz, M.D. Ward, J. Chem. Soc., Dalton Trans. (1992) 3345.
[31] G.K. Labiri, S. Bhattacharya, B.K. Ghosh, A. Chakravorty, Inorg. Chem. 26 (1987) 4324.
[32] R. Hariram, B.K. Santra, G.K. Lahiri, J. Organomet. Chem. 540 (1997) 155.
[33] M.M. Taquikhan, D. Srinivas, R.I. Kureshy, N.H. Khan, Inorg. Chem. 29 (1990) 2320.
[34] B.K. Santra, G.K. Lahiri, J. Chem. Soc., Dalton Trans., (1998) 139.
[35] A.K. Mahapatra, S. Dutta, S. Goswami, M. Mukherjee, A.K. Mukherjee, A. Chakravorty, Inorg. Chem. 25 (1986) 1715.
[36] B.K. Santra, M. Menon, C.K. Pal, G.K. Lahiri, J. Chem. Soc. Dalton Trans. (1997) 1387.
[37] N. Bag, G.K. Lahiri, S. Bhattacharya, L.R. Falvello, A. Chakravorty, Inorg. Chem. 27 (1988) 4396.
[38] B.K. Santra, G.K. Lahiri, J. Chem. Soc., Dalton Trans., (1997) 1883.
[39] A. Pramanik, N. Bag, G.K. Lahiri, A. Chakravorty, J. Chem. Soc., Dalton Trans. (1992) 101.
[40] G.K. Lahiri, S. Bhattacharya, S. Goswami, A. Chakravorty, J. Chem. Soc., Dalton Trans. (1990) 561.
[41] B. Bleaney, M.C.M. O'Brien, Proc. Phys. Soc. London, Sect. B 69 (1956) 1216.
[42] J.S. Griffith, The Theory of Transition Metal Ions, Cambridge University Press, London, 1961, p. 364.
[43] C. Daul, A. Goursot, Inorg. Chem. 24 (1985) 3354.
[44] N.J. Hill, J. Chem. Soc., Faraday Trans. (1972) 427.
[45] C.J. Ballhausen, Introduction to Ligand Field Theory, McGraw-Hill, New York, 1962, p. 99.
[46] S. Bhattacharya, A. Chakravorty, Proc. Indian Acad. Sci., Chem. Sci. 95 (1985) 159.
[47] S. Goswami, R.N. Mukherjee, A. Chakravorty, Inorg. Chem. 22 (1983) 2825.
[48] B.K. Ghosh, A. Chakravorty, Coord Chem. Rev. 95 (1989) 239.
[49] B.P. Sullivan, J.V. Caspar, S.R. Johnson, T.J. Meyer, Organometallics 3 (1984) 1241.
[50] E.S. Dodsworth, A.B.P. Lever, Chem. Phys. Lett. 124 (1986) 152.
[51] M.A. Greaney, C.L. Coyle, M.A. Harmer, A. Jordan, E.I. Stiefel, Inorg. Chem. 28 (1989) 912.
[52] S. Purohit, A.P. Koley, L.S. Prasad, P.T. Manoharan, S. Ghosh, Inorg. Chem. 28 (1989) 3735.
[53] V. Ferreira, R.A. Krause, Inorg. Chim. Acta 145 (1988) 29.
[54] J.W. McDonald, G.D. Friesen, L.D. Rosenhein, W.E. Newton, Inorg. Chim. Acta 22 (1983) 205.
[55] D.T. Sawyer, A. Sobkowiak, J.L. Roberts Jr., Electrochemistry for Chemists, 2nd ed., Wiley, New York, 1995.
[56] A. Pramanik, N. Bag, D. Ray, G.K. Lahiri, A. Chakravorty, Inorg. Chem. 30 (1991) 410.
[57] P. Ghosh, A. Pramanik, N. Bag, G.K. Lahiri, A. Chakravorty, J. Organomet. Chem. 454 (1993) 237.